Integration of an optical system for 3D reconstruction

Filipe Ferreira Monteiro
filipeferreiramonteiro@tecnico.ulisboa.pt

Instituto Superior Técnico, Lisboa, Portugal, Universidade de Lisboa, Lisboa, Portugal

November 2020

Abstract

Given the stone industry vitality to any economy, its continuous progress is of significant interest. To improve their products and industry, the company, Fravizel, desires to use 3D metrology tools in order to obtain 3D models of the stone blocks extracted in quarries. 3D models of the unprocessed stone blocks could be used to optimize intermediary processes and 3D models of the processed stone blocks could be used for advertising.

This thesis offers a solution for the design of 3D scanners that acquires the information required for 3D reconstruction through computer vision. The first scanner consists of integrating an optical system to Fravizel's machines, alleviating the cost of new infrastructures. The second scanner consists of a camera system capable of acquiring images while circling the stone block, for an advertisable gapless high-quality 3D model. The data, the proposed scanners acquire, consists of a set of images required for reconstruction and the calibrations of the image sensors that could increase the efficiency of the reconstruction process.

Both scanner configurations yielded positive yet not ideal data for the reconstruction step. The first scanner obtains 12Mp images and was poorly intrinsically calibrated in 461.14 seconds with a mean-absolute-error of 33.99 pixels. The second scanner obtains 8Mp images and was well intrinsically calibrated in 124.03 seconds with a mean-absolute-error of 0.13 pixels. Pose estimations across both scanners were more reliable using algorithms without RANSAC obtaining correct calibrations with mean-absolute errors of 0.27-0.43 pixels in the first scanner and 0.14-8.87 pixels in the second scanner.

Keywords: Quarry industry, 3D Metrology, 3D Scanner, Computer Vision, Pose Estimation

1 Introduction

Mineral resources are highly sought out recourses generated by natural geological processes. These processes are large scaled, slow, outside the control of humanity and not replicable, making these resources, practically speaking, nonrenewable [1]. Humanity has used mineral resources since pre-historic time. We have continuously evolved and developed the use of more and more mineral resources with such significance that historic periods have been referred to as the stone age, the Bronze Age, and so on, as we updated our methods and technology with newer minerals. Presently we have found applications for most discovered natural resources. Mineral recourses can be categorized based on their application, fuel minerals, industrial minerals and metallic minerals [2].

Limestone is an example of a rock, mostly composed of the mineral calcite, this is a mineral recourse commonly used worldwide in construction, either structurally or decoratively, and in the production of cement, an important building material. In a quarry the limestone is removed from its bedrock in large parallelepiped blocks. These blocks must be processed into an acceptable state, before they can be sold, one of the steps in this process involves cutting the block to remove flaws. Quarries use heavy machinery equipped with saws to cut the stone blocks.

The size and weight of the stone blocks become a hindrance to the advertising and cutting process of the blocks:

- The stone blocks are inspected for flaws, visually by a worker
- The cuts placement is determined visually by a worker.
- The cutting machine is positioned manually by a worker.
- Images of the processed stone blocks poorly advertise the quality of its surface and dimensions.

We intend to take a step towards minimizing these shortcomings using 3D Metrologic technology. Therefore, this thesis statement is: Design and implement a 3D scanning system that optimizes the following 3D reconstruction, improving its efficiency and viability. The main question this thesis aims to answer is:

How effectively does the proposed solution collect the data required for 3D reconstruction?

In order to answer this question, the following complementary questions should also be addressed:

1. What type of scanner is most viable towards replacing the workers visual analysis of the stone blocks?
2. Can the proposed solution be designed around the Fravizel's machine, in order to use the existing structure and functionalities?
3. What other mediums can be used to advertise the blocks?

2 Literary Review

Three-dimensional reconstruction is the process of determining the three-dimensional profile and coordinates of the surface points of an object. The process of collecting the required data for 3D reconstruction is referred to as 3D Scanning. Three-dimensional scanning can be divided into two categories: Methods that required physical interaction with the object, contact scanning, and methods that do not require physical interaction with the object, non-contact scanning [3]. Contact scanning is a straightforward process, the object is fixed to a precision flat surface plate or fixture while a high precision kinematic chain system repeatedly touches the objects surface recording measurements of the location of the kinematic chain's probe to be used as data for the 3D reconstruction. An example of this are the coordinate-measuring machines more commonly called CMM scanners [4]. Contact systems applicability is limited due to its physical approach. The used process requires the mapping of the surface, point by point limiting the speed of the process, the dimensions and resistance of the object.

In order to collect information on an object's shape without physically interaction, non-contact scanners were developed using known properties of several types of emissions such as radiation and sounds by detecting or recording their interaction with the object. Non-contact scanners are divided into two categories, active and passive [5]. Non-contact active systems collect data regarding object's dimensions by generating an emission such as radiation, light or sound at the object and detecting the radiation that passed through the object, such as x-ray techniques or the reflection of the light or sound, such as camera or sonar systems. Time-of-flight, triangulation and phase measurement are examples of methods used to calculate distance or slope distribution of a surface with the detected information from the emissions sent towards the object [6]. The speed of these scanners will be considerably faster than contact scanners given the lack of need to physically interact with the object, but how much faster depends on the method, hardware and the type data collected for the reconstruction. Active scanners are varied in hardware and operating principles, from a simple set up consisting of a digital camera and an emitter acquiring images for reconstruction through triangulation, to more technically specific system such as 3D terrestrial laser scanners based on the various measuring principles mentions above.

Non-contact passive systems collect data regarding object's dimensions by detecting naturally available emissions, such as ambient radiation, reflected by the object. The most practical systems in this category involve image sensors, detecting the ambient radiations in the visible spectrum, through photogrammetric processes [7]. The most common type of passive scanner are basic cameras that acquire simple images of the object, with no use of projections or laser to enhance the data in the images. The reconstruction process is done through triangulation with the camera poses and the corresponding features between the respective acquired images, as shown in Figure 1.

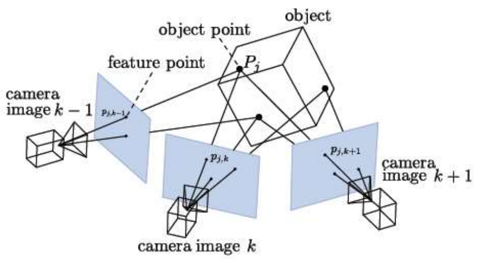

Figure 1: Triangulation through feature matching [8]

Compare to contact and non-contact active scanners, non-contact passive scanner can present some advantages, such as speed, economic cost, operational difficulty, thoroughness and the lack of physical interaction with the object. This concludes that non-contact passive scanners are more suitable to our intended applications.

Image sensors used in passive scanner require two different types of calibrations. An intrinsic calibration to determine the internal parameters of the image sensor and an extrinsic calibration to determine the pose of the image sensor, the internal parameters remain constant while the pose must be estimated for of each image acquisition.

Calibrations are performed considering the pinhole camera model that relates the point's three-dimensional coordinates to the image coordinates. For the pinhole model of optical imaging, the camera equation to obtain a three-dimensional point in the image plane is:

$$\lambda \begin{bmatrix} x \\ y \\ 1 \end{bmatrix} = P \begin{bmatrix} X_w \\ Y_w \\ Z_w \\ 1 \end{bmatrix} = K[R\ t] \begin{bmatrix} X_w \\ Y_w \\ Z_w \\ 1 \end{bmatrix} =$$

$$= \begin{bmatrix} f_x & s & c_x \\ 0 & f_y & c_y \\ 0 & 0 & 1 \end{bmatrix} \begin{bmatrix} r_{11} & r_{12} & r_{13} & t_1 \\ r_{21} & r_{22} & r_{23} & t_2 \\ r_{31} & r_{32} & r_{33} & t_3 \end{bmatrix} \begin{bmatrix} X_w \\ Y_w \\ Z_w \\ 1 \end{bmatrix}$$

Where λ is a nonzero scale factor; (x, y) are the point's coordinates in the image coordinate system; (x_w, y_w, z_w) are the point's coordinates in the world coordinate system; P is the camera matrix composed of $K[R\ t]$.

K is an upper triangular matrix containing the intrinsic parameters, properly referred to as the matrix of the intrinsic camera parameters. The intrinsic parameters, f_x and f_y are the focal lengths in the x-axis and y-axis directions respectively; (c_x, c_y) is the principle point coordinates; and s is a skew parameter that corrects for tilted pixels, safely assumed to be zero for most cameras [7].

R is the 3x3 rotation matrix and t is a 3x1 translation matrix that encodes the orientation and positions of the camera, in the world coordinate system, these are the extrinsic parameters further explained later.

Commonly used today, camera calibrations are based on a technique developed by Zhengyou Zhang. Zhang proposed a new flexible calibration method by using known constraints and assumptions [9][10].

The extrinsic parameters are the external specifications of the image sensor at the time of the acquisitions. These parameters are the position and orientation of the camera's reference frame relative to the world frame. The position is noted in the form of a three-by-one vector containing the cartesian coordinates of the frames origin in relation to the world frame, and the orientation is noted by a three-by-three matrix describing the rotation of the image sensor frame in relation to the world frame.

Determining these extrinsic parameters is accomplished by solving the Perspective-n-Point problem, commonly referred to as PnP problem. Basically, this problem consists of using a set of known 3D points and their corresponding 2D points in the image to estimate the extrinsic parameters of an intrinsically calibrated camera.

To keep within the scope of this thesis, we restricted our search to established and open sourced algorithms, instead of programming algorithms from root. The open source library OpenCV has available several algorithms to solve the PnP problem. The default method used by OpenCV is an iterative algorithm. This algorithm uses n≥4 points, performs an initial estimation for the pose, through a direct linear transform [7], and iterates this estimation using a Levenberg-Marquardt optimization to minimize the reprojection error. The other optional algorithms are based on the following papers for PnP solution:

- P3P algorithm-Complete Solution Classification for the Perspective-Three-Point Problem [11][12].
- AP3P algorithms-An Efficient Algebraic Solution to the Perspective-Three-Point Problem [13].
- EPnP algorithm-An Accurate O(n) Solution to the PnP Problem [11][14].

3 Proposed Solutions

Currently the workers determine the location of the cuts simply by visually inspecting the blocks for flaws. A goal of the proposed system will be to optimize this part of the cutting process. Designing a system to scan and reconstruct a three-dimensional model of stone blocks grants us the ability to analyze the model using computer software. This would allow the quarry to optimize the amount of stone slabbed saved by calculating the positions of the cuts with a higher accuracy. Another objective will be to optimize the advertising quarry method by designing another system capable of scanning a processed block for the acquisition a 3D model for advertisement purposes, this allows quarries to show their customers the full volume and surface quality of their stone blocks if a more comprehensive medium.

Scanner with Linear configuration

This configuration is based on the idea to use the known motion of the Fravizel's cutting machine. The cutting machine consists of a portico which supports the cutting instrument, this portico is installed on top of rails allowing it to move over the stone blocks. The portico rails are encoded and can be used to accurately perform acquisitions at defined intervals of distance. This way the full extrinsic parameters of each image can be easily determined with a single pose estimation, to determine all the extrinsic parameters of the initial acquisition, and the rails motion to easily apply the translation between acquisitions, to the subsequent poses.

Scanner with circular configuration

A 3D model of the finished limestone block would be possible to display on websites through a 3D displayer. This would allow possible buyers to rotate and zoom in and out of the block to obtain a more comprehensive appreciation of its dimensions and surface quality without having to sacrifice either. This configuration is based on this desire to obtain an accurate full gapless 360-degree view of the stone blocks that quarries intend to sell. The pictures are obtained with cameras positioned in a circle around the object, oriented towards the object, this ensures that all surfaces are captured and that there is significant overlap between consecutive cameras perspectives.

To test initial designs and functions two Trust Exis webcams were used as image acquisition devices for small scaled simulations of configurations corresponding to desired applications. To simulate a small-scale version of the first configuration (linear movement), the cameras were connected to one personal computer via USB ports and were accessed via MATLAB software installed with the MATLAB support package for USB webcams. A MATLAB script was created to control the triggering of the cameras. In this configuration, the acquisition of images needs to be synchronized between the cameras to ensure each pair of images corresponds to the same position in the portico's rail, in the real scale application. The triggering method needs to be highly responsive to ensure the image pairs are captured at consistently regular specified intervals. To test the viability of this configuration the MATLAB scripts accomplished two functions triggering the cameras and timing the triggers. The results of this script allows to conclude that while MATLAB can be used to control and trigger multiple cameras, using one computer to send the triggering signal results in significant delays between the cameras, making it impossible to synchronize the acquisition of images between multiple cameras. Also, while the Trust Exis webcams, are a good option to test the viability and properties of image acquisition systems, they produce images with a very low resolution, resulting in a low-quality three-dimensional model. Therefore, to improve the quality of the reconstructed model, images with higher resolutions are also required.

The single-board computers developed by the Raspberry Pi foundation

[15] have optional accessories and modules, such as an eight-megapixel camera module [16]. Since they are computers, however basic, these Raspberry Pis are a very flexible and easy to use tool. They can be used as camera controllers, signal generators and more, allowing a good degree of flexibility for the purpose of testing solutions to our designs. For our purposes, these computers need only enough processing power to manage and trigger one camera, therefore single-board computers are an appropriate cost-effective choice.

Using a Raspberry Pi model 3 B+, as a controller for a V2 eight-megapixel camera module, establishes the optical sensor to be used in the following small-scale simulations of the scanner configuration designs. In these simulations, the scanned object is a common pavement limestone, as they are a good small-scale approximation of the quarry's limestone block, given that they were a small piece of what was once before a large limestone block. A single camera set up is used to test the cameras optical viability and the Raspberry Pi capabilities.

The Raspberry Pi was also used to test the multiple cameras synchronicity. Both cameras were set up to be triggered externally by the same signal generated by the Raspberry Pi. The generated signal was set to trigger acquisition every 1 second. Both cameras were aimed to a browser stopwatch to obtain a direct timestamp for the acquisitions. The results were organized in the following Table 1, allowing us to conclude that using an external signal to trigger the cameras results in a very satisfying synchronicity.

Table 1: Camera trigger's timestamps

Cam 1 (sec)	2.253	3.252	4.251	5.247	6.247
Cam 2 (sec)	2.253	3.252	4.251	5.247	6.247

Proposed 3D Scanners

The proposed 3D scanner with linear configuration, consists of a pair of cameras attached to beams on the mobile portico structure and triggered by the same signal generated by its encoder, as the portico moves. The cameras are equipped with 1.1-inch format 12-megapixel optical lenses with a broad field of view and a case to protect it from weather and harsh working conditions.

The designed 3D scanner with circular configuration, is a small-scale version of the proposed scanner. This small-scale scanner consists of a single camera supported by a kinematic chain and a servomotor, a common pavement limestone rock is used as a proxy to the quarry large limestone blocks. The camera used is a 8-megapixels Pi Camera controlled by a Raspberry Pi. The kinematic chain is composed of three 3D printed joints, a prismatic joint allowing vertical translations, a rotational joint allowing rotation around a vertical axis, turning the camera left and right and another rotational axis allowing rotation around a horizontal axis, tilting the camera up and down. The servomotor is a continuous servo, capable of 360-degree rotations. This scanner maintains the camera, supported by the previously described structure, in a static position while using the raspberry pi to control the camera for image acquisition and the servo to rotate the object. The object's rotation is accomplished by a defined amount of degrees between image acquisitions. To obtain a full reconstruction without gaps, the set of images used must view the object from enough directions as to eliminate blind spots and to ensure enough overlap for proper reconstruction.

Intrinsic Calibrations

For 3D reconstruction an optional input are the cameras intrinsic parameters, calculated through calibration. The cameras were calibrated using established tools or programmed functions. The MATLAB software comes installed with an app named Camera Calibrator for easy calibrations, later a python script using pre-built OpenCV functions was used to calibrate the cameras.

MATLAB's app, Camera Calibrator, receives two inputs: a set of images of a chessboard pattern, taken from the camera to be calibrated; and the size of the patterns squares in metric units. The chessboard pattern is supplied by the MATLAB documentation. The app performed all the calculations using the identifiable corners of the pattern and outputted the intrinsic parameters and mean absolute error.

Using OpenCV functions through Python an intrinsic calibration is accomplished through the same inputs. The script is composed of three basic functions, one function uses the dimension of the chessboard pattern square to construct a matrix of three-dimensional coordinates of the identifiable points from the pattern, the second function analyses each image of the chessboard pattern and construct a matrix with the two-dimensional image coordinates of the corresponding points and the final function uses both these matrices to estimate the intrinsic parameters. The mean absolute reprojection error is also calculated using the estimated intrinsic parameters.

Extrinsic Calibrations

Estimating the poses of the cameras for each image acquisition can be accomplished by solving the Perspective-n-Point problem. OpenCV function were used in a Python script to estimate the poses of the camera for the corresponding images. This calibration process needs as inputs, the intrinsic parameters, a single image and the three-dimensional coordinates of the identifiable points in the respective image. The notion being the correspondence between the three-dimensional coordinates and the two-dimensional image coordinates of a set of points from the image provided, would allow the estimation of the pose. The points were provided in one of two ways, either through the same chessboard pattern used in intrinsic calibration or using four Aruco markers, which are a set of different identifiable square patterns. The image of the pattern of choice was acquired and the chessboard or Aruco markers positions was manually measured and supplied to the script in the correct matrix form. The script outputted the estimated poses and the corresponding mean absolute error, the estimated poses were displayed through a 3D plot for added verification and visualization.

4 Results

The proposed scanner with a linear configuration for the improvement of the stone cutting process, acquires a set of images with a resolution of (4112, 3008) pixels each. The set of images come with an interval of 15 centimeters, along the cutting machines rail, between acquisitions. Through Python using OpenCV functions, this system was intrinsically stereo calibrated using 100 images, containing the chessboard pattern, for each camera, the estimated calibration resulted in a mean absolute reprojection error of 33.99 pixels. The MATLAB stereo calibration app estimation resulted in a mean absolute reprojection error of 0.8888 pixels. It was theorized that the set of images used for calibration had the chessboard pattern cover a limited portion of the camera's large field-of-view resulting in poor calibrations.

The extrinsic calibration was performed using the chessboard pattern with the four algorithms mentioned in section 2, with and without RANSAC. The resulting mean absolute reprojection errors are summarized in the following Figure 2.

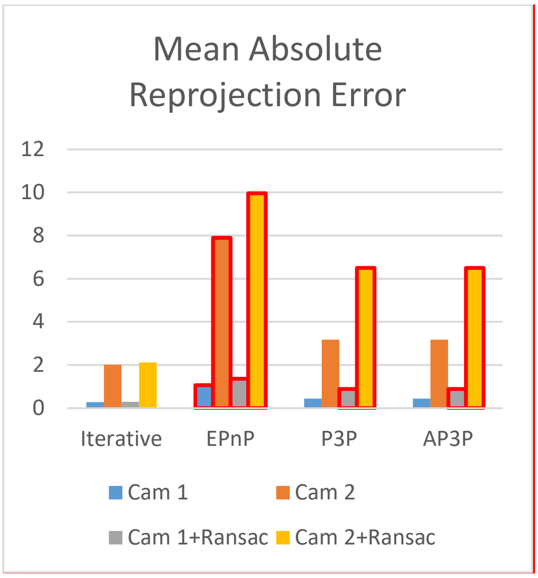

Figure 2: Linear Scanner Pose estimation Reprojection error
Wrong Pose estimations highlighted in red

From Figure 2 we can see that RANSAC has induced wrong estimation for the P3P and AP3P algorithms while using 87% and 90% of points respectively. The iterative algorithms, both with and without RANSAC, obtained a proper estimation with significant lower error than the estimation performed by the P3P and AP3P algorithms without RANSAC. The Efficient-PnP algorithms performed poorly, resulting in wrong estimations with and without RANSAC.

The proposed scanner with a circular configuration for the improvement of the advertising process, acquires a set of images with a resolution of (3280, 2464) pixels each. The set of images comes with an interval of 30 degrees, around the object, between acquisitions. Through Python using OpenCV functions, this system was intrinsically calibrated using 78 images, containing the chessboard pattern. The estimated calibration resulted in a mean absolute reprojection error of 0.1336 pixels. The MATLAB calibration app estimation resulted in a mean absolute reprojection error of 0.7676 pixels.

The extrinsic calibration was performed using the four algorithms mentioned in section 2, with and without RANSAC, on the four Aruco markers and the chessboard pattern. The resulting mean absolute reprojection errors are summarized in the following Figure 3.

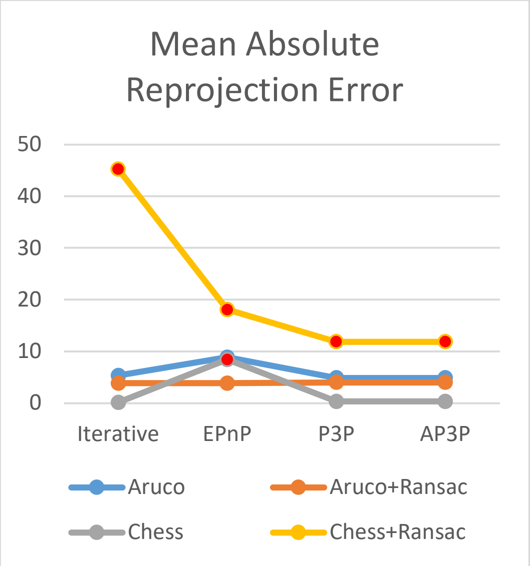

Figure 3: Circular Scanner pose estimations reprojection errors
Wrong pose estimation highlighted in red

Considering the calibrations performed without Ransac, while the points from the Aruco markers were non-coplanar and more varied coordinates-wise, the estimation resulted in higher mean absolute and root mean square reprojection errors compared to the correct calibrations using the chessboard pattern. Using Ransac resulted in entirely wrong poses across all algorithms applied on the chessboard pattern, using only 11% of points with Iterative or Efficient-PnP algorithms, and using 96% of points with P3P and AP3P. However, the Aruco markers seem to have fared better managing to estimate with a decent approximation while only using 42% of the points with Iterative or Efficient-PnP algorithms and 39% of the points with P3P and AP3P algorithms.

Overall all algorithms with or without Ransac when applied on the Aruco markers, have resulted in the correct pose albeit with lower accuracy indicated by the reprojection errors, while the chessboard pattern has with some algorithms resulted in entirely wrong poses, showing however great accuracy when it does work properly.

Given that a small number of poses and patterns were used to test the algorithms, these results might not reflect the cause of their limitations or general behavior.

5 Conclusions

The scanning system proposed to improve upon a quarry's cutting process was design to be incorporated into the existing Fravizel's cutting machine used by quarries. Succinctly, a non-contact passive scanner consists of a system of cameras aimed at the target object to acquired images of the object from different perspectives. For this system, a pair of stereo calibrated cameras was installed onto the cutting machine, using its infrastructure and mechanisms to support, move and trigger the cameras as synchronously as possible. The resulting images from a test scan were very clear and synchronized to the centisecond between the camera pair.

This scanning system, consisted of two Dalsa's Genie Nano C4020 cameras and accessories, such as protective housing, costing a total of 13 575,39€. This linear scanner produced scans of twelve-megapixels synchronized images, and while the intrinsic calibration was sub-optimal the extrinsic calibration produced decent results with some algorithms, notably P3P algorithms. The intrinsic calibration took 461,13 seconds to estimate the intrinsic values, resulting in high mean absolute reprojection errors, 38,55 and 29,43 pixels for camera 1 and 2 respectively, and badly estimated distortion coefficients can be seen by the undistorted images in Figure 78. This can be improved by using a set of images with the detectable chessboard pattern more evenly distributed around the field-of-view, especially the edges of the field-of-view for better distortion coefficients estimation.

Considering the use of a sub-optimal intrinsic calibration, the iterative algorithms resulted in correct extrinsic calibrations, with and without RANSAC, showing low mean absolute reprojection errors of 0.27-0.29 and 2.01-2.12 pixels for camera 1 and camera 2 respectively, while P3P-based algorithms only estimated extrinsic parameters correctly without RANSAC, showing mean absolute reprojection errors of 0.43 and 3.17 pixels for camera 1 and camera 2 respectively. The incorrectly estimated extrinsic parameters, using P3P-based algorithms, show mean absolute reprojection errors of 0.89 and 6.50 pixels for camera 1 and camera 2 respectively. The efficient-PnP algorithms failed to properly estimate extrinsic parameters with and without RANSAC, showing for camera 1 and camera 2, mean absolute reprojection errors of 1.07 and 7.9 pixels without RANSAC and 1.36 and 9.97 pixels with RANSAC respectively. However, with proper intrinsic values they might function properly conveying reliably to the extrinsic calibration process across all algorithms and circumstances. Considering that intrinsic calibration is only required if the cameras internal properties are altered between scans and that extrinsic calibration are required for each scan, the time consumption of a scan boils down to the time it takes to intrinsically calibrate the cameras divided by the number of scans performed, plus the time to acquire the images and perform the extrinsic calibration for each scan. Considering that the intrinsic calibration took no longer than 8 minutes and the extrinsic calibration slightly less than 6 seconds, the scanning process is accomplished nearly in the same time it takes to move the Fravizel's cutting machine over the stone blocks.

A scanning system with a circular movement was proposed to acquire a set of pictures from perspectives in a 360-degree motion around the object for a full high-quality reconstruction to improve the quarries advertising process. A small-scale version of this system was constructed, where a single camera remains stationary while the object is rotated, through the use of a servo motor, at consistent intervals between image acquisitions, simulating the motion of the camera itself around the object.

This scanner consisted of a Raspberry Pi 3B+, a Pi Camera v2, a continuous servo motor and a 3D printed kinematic chain, producing scans of eight-megapixel images. The camera was properly intrinsically calibrated, in 124,03 seconds, showing mean absolute reprojection error of 0,13 pixel. Several methods were used to achieve accurate extrinsic calibrations, the chessboard pattern or four Aruco markers were used to generate world to image coordinate correspondences while different algorithms were used for comparison. The Aruco markers resulted in proper extrinsic calibrations across all algorithms used with and without RANSAC, albeit with higher mean absolute reprojection errors, of 3.86 and 4.02 pixels respectively, when compared to extrinsic calibrations accomplished without RANSAC using the chessboard pattern, which resulted in mean absolute reprojection errors within 0.14 to 0.29 pixels, with the exception of the efficient-PnP algorithm which incorrectly estimated extrinsic parameter, showing a mean absolute reprojection error of 8.42 pixels.. Using RANSAC on the chessboard pattern improperly estimated extrinsic parameters with all algorithms, resulting in mean absolute reprojection errors of 45.2, 18.07 and 11.85 pixels for iterative, efficient-PnP, and P3P-based algorithms respectively.

While the proposed scanner's data acquisition viability yielded positive results, it also showed room for improvement in the form of possible next steps and optimizations. Considering these scanners are a first step in a contribution to the quarry industry, some of the possible improvements are described subsequently.

- **Adding Second stereo camera pair for linear scanner** - The proposed scanner's physical configuration leaves a portion of the stone blocks unreconstructed, corresponding to blind spots in the camera's fields-of-view. Adding another stereo pair of cameras would eliminate the blind spot.
- **Establish Real scale Circular Configuration** - Given that the proposed small-scale circular scanner showed viability in obtaining the data for the reconstruction of good quality 3D models absent of blind spots, the next step would be to design a full-scale version of this scanner and implement it on the processed stone blocks.
- **Use Surface Enrichment** - 3D reconstruction through images is based on detectable features on the surface of the object across the set of images, the ability to reconstruct and the quality of the model is related with the amount and quality of these features. Considering the uniformity of limestone blocks texture and color-wise, a projector could be used to project noise function-based patterns onto the stone blocks to enrich possibly featureless surfaces, as shown in [17].

References

[1] S. A. Nelson, "Mineral Resources." https://bit.ly/2H8ntPc (accessed Sep. 25, 2020).

[2] L. Johansson Westholm and D. Alderton, *Mineral Resources*. Elsevier Inc., 2015.

[3] F. Franceschini, M. Galetto, D. Maisano, and L. Mastrogiacomo, “Large-scale dimensional metrology (LSDM): From tapes and theodolites to multi-sensor systems,” *Int. J. Precis. Eng. Manuf.*, vol. 15, no. 8, pp. 1739–1758, 2014, doi: 10.1007/s12541-014-0527-2.

[4] E. Savio, “Coordinate Measuring Machine,” in *CIRP Encyclopedia of Production Engineering*, 2019.

[5] B. Curless, “From Range Scans to 3D Models,” *Comput. Graph.*, vol. 33, no. 4, pp. 38–41, 1999, doi: 10.1145/345370.345399.

[6] J. Butime, I. Gutierrez, L. G. Corzo, and C. F. Espronceda, “3D reconstruction methods, a survey,” *VISAPP 2006 - Proc. 1st Int. Conf. Comput. Vis. Theory Appl.*, vol. 2, pp. 457–463, 2006, doi: 10.5220/0001369704570463.

[7] R. Hartley and A. Zisserman, *Multiple View Geometry in computer vision*, Second. 2004.

[8] “sfm — openMVG library.” https://openmvg.readthedocs.io/en/latest/openMVG/sfm/sfm/ (accessed Oct. 17, 2020).

[9] Z. Zhang, “A flexible new technique for camera calibration,” *IEEE Trans. Pattern Anal. Mach. Intell.*, vol. 22, no. 11, pp. 1330–1334, 2000, doi: 10.1109/34.888718.

[10] W. Burger, “Zhang’s Camera Calibration Algorithm: In-Depth Tutorial and Implementation,” *Tech. Rep.*, p. 55, 2016, doi: 10.13140/RG.2.1.1166.1688.

[11] X. X. Lu, “A Review of Solutions for Perspective-n-Point Problem in Camera Pose Estimation,” 2018.

[12] X. Gao, X. Hou, J. Tang, and H. Cheng, “Complete Solution Classification for the Perspective-Three-Point Problem,” vol. 25, no. 8, pp. 930–943, 2003.

[13] T. Ke and S. I. Roumeliotis, “An efficient algebraic solution to the perspective-three-point problem,” *Proc. - 30th IEEE Conf. Comput. Vis. Pattern Recognition, CVPR 2017*, vol. 2017-Janua, pp. 4618–4626, 2017, doi: 10.1109/CVPR.2017.491.

[14] V. Lepetit, F. Moreno-Noguer, and P. Fua, “EPnP: An accurate O(n) solution to the PnP problem,” *Int. J. Comput. Vis.*, vol. 81, no. 2, pp. 155–166, 2009, doi: 10.1007/s11263-008-0152-6.

[15] “Raspberry Pi hardware - Raspberry Pi Documentation.” https://bit.ly/3dC5TyM (accessed Sep. 30, 2020).

[16] “Camera Module - Raspberry Pi Documentation.” https://bit.ly/3o3Ri3V (accessed Sep. 30, 2020).

[17] A. Koutsoudis, G. Ioannakis, B. Vidmar, F. Arnaoutoglou, and C. Chamzas, “Using noise function-based patterns to enhance photogrammetric 3D reconstruction performance of featureless surfaces,” *J. Cult. Herit.*, vol. 16, no. 5, pp. 664–670, 2015, doi: 10.1016/j.culher.2015.01.008.